# Nature of the state of stress produced by xenon and some alkali iodides when used as pressure media

K. Asaumi and A. L. Ruoff
*Department of Materials Science and Engineering, Bard Hall, Cornell University, Ithaca, New York 14853-1501*
(Received 8 April 1985)

The ruby $R_1$ and $R_2$ line splitting was studied as a function of pressure to 55 GPa in xenon and 70 GPa in three alkali iodides. The ruby $R_1$ and $R_2$ line splitting within the xenon medium was found to remain almost constant up to 55 GPa, while in the case of alkali iodide crystals the splitting was found to increase with increasing pressure and amounted to twice as much at 70 GPa as at 0 GPa. This shift in the splitting has been related to the nonhydrostatic component of the stress and provides a method for measuring the compressive yield stress.

Since the introduction of the ruby high-pressure scale and the use of methanol-ethanol (4:1) as a hydrostatic pressure medium to 10 GPa by Piermarini *et al.*,[1-3] the diamond anvil cell has become a highly popular pressure apparatus for various studies including x-ray, optical, and electrical resistance measurements.[4]

Though the methanol-ethanol (4:1) mixture[2] has been used widely for many high-pressure studies, there is a need to expand the hydrostatic range up to the highest pressure attainable. Experimentally, four potential ways of studying the degree of hydrostaticity of a pressure medium are as follows: (1) measuring the pressure at various points using ruby chips distributed within a gasket hole and relating, if possible, the pressure gradient to the nonhydrostatic stress component, (2) knowing the effect of the nonhydrostatic components of stress on the full width at half maximum (FWHM) of the ruby fluorescence profile and measuring FWHM, (3) measuring the lattice parameter of, say, a cubic crystal within the medium, as a function of angle relative to the loading direction and relating this to the stress components, and (4) knowing the effect of deviatoric stresses on the splitting between the ruby $R_1$ and $R_2$ fluorescence lines and measuring this shift. In case (1) the nonuniformity of the mean normal stress (pressure) is being measured. The resultant pressure gradient can be related to the nonhydrostatic component of the stress.[5] It should be noted that it is possible to have a nonhydrostatic stress without a gradient of the mean normal stress. A relationship between FWHM of the ruby fluorescence peak and nonhydrostatic stress components was noted by Piermarini, Block, and Barnett.[6] The relationship between the angular dependence of the lattice parameter and the nonhydrostatic component of the stress has been described by Ruoff,[7] and such measurements have been made by Kingsland and Bassett.[8] The existence of a shift of the difference between the $R_1$ and $R_2$ peak positions in a pressure gradient has been noted earlier.[9,10] A relationship between deviatoric stress and the splitting between the ruby $R_1$ and $R_2$ fluorescence lines is developed in the present paper.

Some pressure media, so far reported to be quasihydrostatic above the methanol-ethanol limit (10 GPa) are solid rare gases (Xe, Ar, Ne, and He),[11-13] solid nitrogen,[14] and solid hydrogen.[15]

We have recently investigated the effect of very high pressure on xenon[12,16] to 55 GPa and on some alkali iodide crystals[17-20] to about 70 GPa. In the present experiments we observed the pressure effect on the splitting of the $R_1$ and $R_2$ lines of the ruby embedded within these samples.

The diamond anvils used in the present study were 0.23 carat with 0.5—0.7 mm cross-sectional diameter truncated faces. A stainless-steel gasket with 200-$\mu$m thickness was preindented to 80 $\mu$m thick and a 50-$\mu$m hole was drilled at the center of the preindented gasket. Several ruby chips of 10—20 $\mu$m size were distributed within the gasketed hole along with the sample of Xe, CsI, RbI, or KI. Ruby chips were excited by a He-Cd laser (441.6 nm) and the fluorescence emission spectrum was dispersed using a grating monochromator. Pressures were calibrated using a revised ruby scale determined by Mao *et al.*[21]

Figures 1—4 show the pressure dependence of the splitting (peak-to-peak) between the $R_1$ and $R_2$ fluorescence lines of ruby for Xe, CsI, RbI, and KI at room temperature. (If centroid-to-centroid splittings are used, the shift

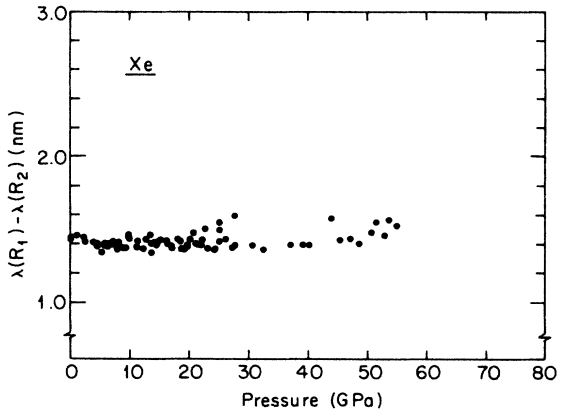


FIG. 1. Peak-to-peak splitting of ruby $R_1$ and $R_2$ fluorescence lines as a function of pressure within the xenon pressure medium.

 

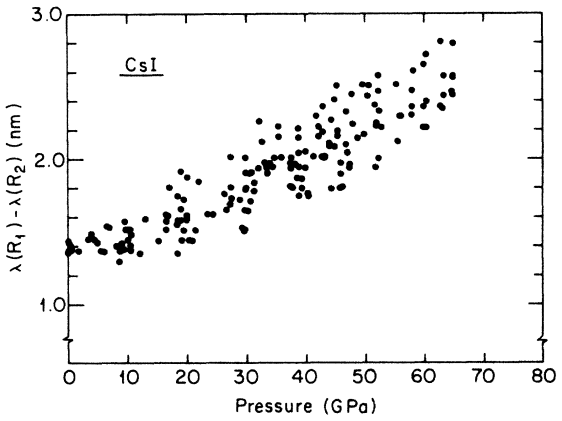


FIG. 2. Ruby $R_1$ and $R_2$ peak-to-peak splitting within the CsI pressure medium.

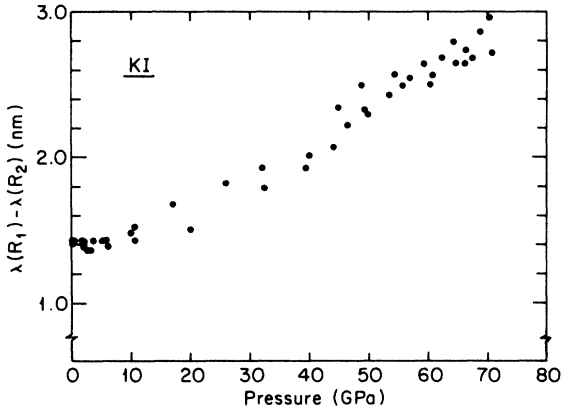


FIG. 4. Ruby $R_1$ and $R_2$ peak-to-peak splitting within the KI pressure medium.

with pressure is slightly larger.) An example of ruby fluorescence profiles for CsI is shown in Fig. 5. In the case of the xenon medium the splitting is almost constant up to 55 GPa. This is consistent with the earlier work on xenon up to 30 GPa by Liebenberg.[11] The splitting of ruby $R_1$ and $R_2$ fluorescence lines embedded within CsI, RbI, and KI (Figs. 2—4) increases gradually with increasing pressure from its initial value 1.4 nm (0 GPa) to about 2.8 nm at 70 GPa. Though the data points are fairly scattered, peak splittings in these figures (Figs. 2—4) show almost the same trend and are quite different from those of xenon. We will show shortly that the shift of $\lambda(R_1)-\lambda(R_2)$ with pressure is a result of nonhydrostatic stresses. We expect the stress state to be of the form[7]

$$\begin{bmatrix} P+2\sigma_0/3 & 0 & 0 \\ 0 & P-\sigma_0/3 & 0 \\ 0 & 0 & P-\sigma_0/3 \end{bmatrix},$$

where $\sigma_0$ is the yield stress of the solid at the pressure $P$. The pressure difference across a CsI sample has been measured by measuring the energy-band gap across a sample of CsI when it varies from yellow to red and using the band gap versus pressure relationship[17] to obtain the pressure variation across the sample. The thickness at pressure was obtained by measuring the sample area at pressure and after unloading and by measuring the sample area and thickness after unloading and using the measured equation of state.[17,18] Then using the relation[5]

$$dP/dr = -\sigma_0/h \ , \tag{1}$$

where $r$ is the radius and $h$ is the sample thickness, we find that $\sigma_0$ is 1.4 GPa at a pressure of 37 GPa. In general we can expect that the yield stress increases with pressure according to

$$\sigma_0=\sigma_{00}(1+C_0'P/C_0) \ , \tag{2}$$

where $C_0$ is an effective elastic constant at zero pressure and $C_0'$ is the first derivative of that elastic constant at zero pressure.[22] If $C_0'P/C_0 \gg 1$, then $\sigma_0$ is expected to be proportional to the pressure. Making this assumption we

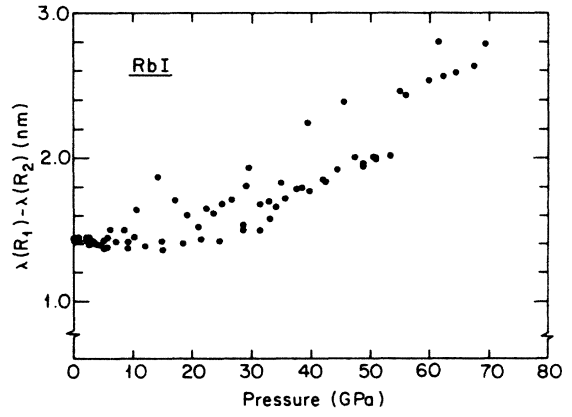


FIG. 3. Ruby $R_1$ and $R_2$ peak-to-peak splitting within the RbI pressure medium.

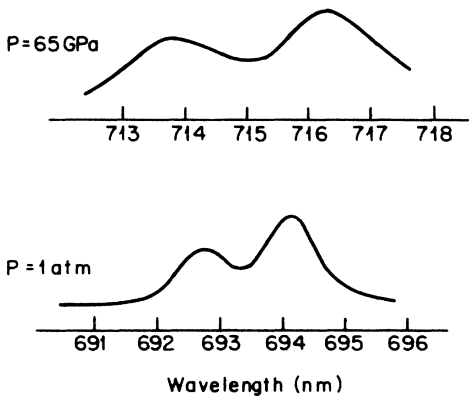


FIG. 5. Ruby fluorescence spectra at $P=1$ atm and $P=65$ GPa for the CsI pressure medium. Different intensity scales are used. Aperture settings may be different so peak width comparisons may not be significant.

have for CsI

$$\sigma_0/P = 1.3/3.7$$

or

$$\sigma_0 = 0.04P \ . \tag{3}$$

Using this along with our present results for CsI which can be approximated by

$$P = 50[\lambda(R_1) - \lambda(R_2) - 1.4] \ , \tag{4}$$

we have

$$\sigma_0 = K[\lambda(R_1) - \lambda(R_2) - 1.4] \ , \tag{5}$$

with $K$ being 2 GPa/nm. Further studies are needed to obtain a better value of $K$; such studies should include the dependence on the orientation of the ruby crystal in the diamond cell.

There also are significant differences in the quality of the x-ray diffraction pattern for these different materials. In the case of xenon, sharp diffraction peaks of (111), (200), (220), (311), and (222) were obtained to the highest pressure of 33 GPa.[16] On the contrary, in the x-ray diffraction studies of CsI,[19,20] for example, significant broadening of the (110), (200), and (211) peaks was observed, and the weak (200) line disappeared above 10 GPa. Both of these solids are being plastically deformed during pressurization, and this is expected to cause line broadening.[23]

The extent of the x-ray line broadening and of the shift of the difference of $\lambda(R_1) - \lambda(R_2)$ depends on the history of strain rate, strain, and temperature. If the plastic strain and the strain rate are small and the temperature is near or above half the melting temperature, then the effect due to plastic deformation may be small, while if the reverse is true, it can be expected to be large. In our samples at 30 GPa, pressure changes of about 2.5 GPa were made about every thirty minutes, with a resultant strain rate of about $10^{-4}$ sec$^{-1}$. In the x-ray experiments the strain rates were about $2 \times 10^{-6}$ sec$^{-1}$. There should be a crossover from high-temperature creep when the reduced temperature (relative to the melting temperature) decreases below about 0.5.

Heavily plastically deformed crystalline materials may undergo recrystallization (and a corresponding stress relaxation and peak narrowing) at temperatures as low as $T/T_M = 0.33$ when $T_M$ is the melting temperature. At reduced temperatures below 0.33, the yield stress is usually nearly independent of temperature.[24] Therefore, recrystallization of CsI ($T_M = 894$ K), RbI ($T_M = 959$ K), and KI ($T_M = 915$ K) is unlikely even at room temperature and pressure and even more unlikely at high pressure because the melting temperature increases with pressure. Thus in the low-temperature deformation regime (below $T/T_M = 0.33$), we expect a sizeable nonhydrostatic component of stress.

Another pressure medium often used in the diamond anvil cell is nitrogen which solidifies at 2.4 GPa at room temperature; it is chemically inactive and readily available. The hydrostaticity and the Raman shift of solid nitrogen at room temperature were reported by LeSar *et al.*[14] They also measured the splitting between ruby $R_1$ and $R_2$ fluorescence lines and reported that, though the splitting between $R_1$ and $R_2$ remains almost constant below 13 GPa (29 cm$^{-1}$ in the wave-number scale), it began to increase above that pressure and amounted to almost 35 cm$^{-1}$ (which corresponds to 1.7 nm on the wave-length scale) at 30 GPa. In the case of $N_2$ which melts at 300 K at a pressure of 2.4 GPa, it is estimated from the Simon equation[25] that the following melting pressures and temperatures exist: 8.9 GPa, 600 K; 18.5 GPa, 900 K. Thus, at room temperatures, rapid stress relaxation will still occur at 8.9 GPa ($T/T_M = 0.5$) but will be unlikely at pressures as high as 18.5 GPa ($T/T_M = 0.33$). So nonhydrostatic conditions should prevail at the higher pressures.

For hydrogen there is little or no shift of $\lambda(R_1) - \lambda(R_2)$ with pressure between 0 and 62.8 GPa.[15] Based on the Simon equation,[25] the melting pressure at 900 K is 38.3 GPa, and we could expect nonhydrostatic stresses to be in evidence at higher pressures; the highest pressure corresponds to a melting temperature of 1195 K and so $T/T_M = 0.25$, and thus we would expect a shift of $\lambda(R_1) - \lambda(R_2)$ which is not evident.

Xenon has the following melting points: 900 K, 3.7 GPa; 1200 K, 6.1 GPa.[25] Hence, we would expect that stress relaxation should not occur at pressures above 5 GPa or so, resulting in a shift at somewhat higher pressures. Probably the yield stress, $\sigma_0$, of both hydrogen and xenon is very small even at very high pressures (i.e., even in the regime of low reduced temperatures) so the shift becomes insignificant; why this is so is an interesting scientific question. The present study suggests that xenon is a good material to use as a pressure medium at high pressure (50 GPa).

We acknowledge the support of the National Science Foundation through Grant No. DMR-83-05798. We also are thankful for the use of the facilities of the Cornell Materials Science Center which are supported by the National Science Foundation. We acknowledge helpful conversations with William Bassett and Yogesh Vohra.

[1]J. D. Barnett, S. Block, and G. J. Piermarini, Rev. Sci. Instrum. **44**, 1 (1973).

[2]G. J. Piermarini, S. Block, and J. D. Barnett, J. Appl. Phys. **44**, 5377 (1973).

[3]G. J. Piermarini, S. Block, J. D. Barnett, and R. A. Forman, J. Appl. Phys. **46**, 2774 (1975).

[4]A. Jayaraman, Rev. Mod. Phys. **55**, 65 (1983).

[5]K. S. Chan, T. L. Huang, T. A. Grzybowski, T. J. Whetten, and A. L. Ruoff, J. Appl. Phys. **53**, 6607 (1982).

[6]G. J. Piermarini, S. Block, and J. D. Barnett, J. Appl. Phys. **44**, 5377 (1973).

[7]A. L. Ruoff, J. Appl. Phys. **46**, 1389 (1975).

[8]G. L. Kingsland and W. A. Bassett, Rev. Sci. Instrum. **47**, 130 (1976).

[9]D. M. Adams, R. Appleby, and S. K. Sharma, J. Phys. E **9**, 1140 (1976).
[10]J. M. Besson and J. P. Pinceaux, Rev. Sci. Instrum. **50**, 541 (1979).
[11]D. H. Liebenberg, Phys. Lett. **73A**, 74 (1979).
[12]K. Asaumi, T. Mori, and Y. Kondo, Phys. Rev. Lett. **49**, 837 (1982).
[13]P. M. Bell and H. K. Mao, Carnegie Inst. Washington Yearb. **80**, 404 (1980–1981).
[14]R. LeSar, S. A. Ekberg, L. H. Jones, R. L. Mills, L. A. Schwalbe, and D. Schiferl, Solid State Commun. **32**, 131 (1979).
[15]H. K. Mao and P. M. Bell, Carnegie Inst. Washington Yearb. **78**, 659 (1978–1979).
[16]K. Asaumi, Phys. Rev. B **29**, 7026 (1984).
[17]K. Asaumi and Y. Kondo, Solid State Commun. **40**, 715 (1981).
[18]K. Asaumi, T. Suzuki, and T. Mori, Phys. Rev. B **28**, 3529 (1983).
[19]T. L. Huang and A. L. Ruoff, Phys. Rev. B **29**, 1112 (1984).
[20]K. Asaumi, Phys. Rev. B **29**, 1118 (1984).
[21]H. K. Mao, P. M. Bell, J. W. Shaner, and D. J. Steinberg, J. Appl. Phys. **49**, 3276 (1978).
[22]J. O. Chua and A. L. Ruoff, J. Appl. Phys. **46**, 4659 (1975).
[23]C. S. Barrett and T. B. Massalski, *Structure of Metals* (McGraw-Hill, New York, 1966), p. 453.
[24]W. F. Smith, *Structure and Properties of Engineering Alloys* (McGraw-Hill, New York, 1981), p. 150.
[25]S. E. Babb, Jr., Rev. Mod. Phys. **35**, 400 (1963).